

A Control Structure for Fast Harmonics Compensation in Active Filters

J. H. Allmeling

EEH – Power Systems Laboratory
Swiss Federal Institute of Technology (ETH Zurich)
8092 Zurich, Switzerland

Abstract— Shunt active filters are a means to improve power quality in distribution networks. Typically, they are connected in parallel to disturbing loads in order to reduce the injection of non sinusoidal load currents into the utility grid. The high power active filter investigated in this paper is based on a PWM controlled voltage source inverter. Its inner current control is realized with a dead-beat controller that allows fast tracking of stochastically fluctuating load currents. For the mitigation of stationary load current harmonics, an outer control loop is required that compensates for the persistent phase error caused by the delay of the inner loop.

The outer loop developed in this paper is based on integrating oscillators tuned to the major load current harmonics. Mathematically, they are equivalent to I-controllers in rotating reference frames. Some of these oscillators are located within a closed control loop. For frequencies where the feedback would excite grid resonances they are placed in a prefilter with phase shifting elements. Since all oscillators share a common feedback full selectivity of the harmonic analysis is achieved. For every harmonic the degree of compensation can be adjusted individually.

In addition to the oscillators, a direct path is provided that feeds forward the load current to the inner control loop. Thus, load current transients can be tracked with the full speed of the dead-beat controller. The direct path does not affect the harmonic analysis performed by the oscillators

I. INTRODUCTION

DISTURBING loads like arc furnaces and thyristor rectifiers draw fluctuating and harmonic currents from the utility grid. These non sinusoidal currents cause a voltage drop across the finite internal grid impedance, and the voltage waveform in the vicinity becomes distorted. Hence, the normal operation of sensitive consumers is jeopardized.

Active filters are a means to improve the power quality in distribution networks. In order to reduce the injection of non sinusoidal load currents shunt active filters are connected in parallel to disturbing loads. Fig. 1 outlines the electrical circuit for the active filter investigated in this paper. Its main component is a voltage source inverter (VSI) with DC link capacitors. The VSI is connected to the point of common coupling (PCC) via a decoupling inductor that is usually the leakage inductance of a transformer. The configuration is identical with an advanced static var compensator.

In order to meet the high power demands and to increase the resulting pulse frequency compared to 2-level topologies a 3-level neutral-point clamped inverter has been employed. The commands for the semiconductor switches are generated using pulse width modulation (PWM) with symmetrical triangular carriers. Since in

high power applications the semiconductor switching frequency is limited to a few hundred hertz, an additional passive filter is required to remove the strong current ripple produced by the VSI.

The purpose of the active filter is to compensate transient and harmonic components of the load current i_L so that only fundamental frequency components remain in the grid current i_N . Additionally, the active filter may provide the reactive power consumed by the load. The control principle for the active filter is rather straightforward: The load current i_L is measured, the fundamental active component is removed from the measurement, and the result is used as the reference for the VSI output current i_{VSI} .

The required fast current tracking capability can be implemented using the dead-beat controller described in [1]. To avoid VSI generated harmonics in the current measurement, the currents are sampled at the tips and zero crossings of the triangular PWM carriers. At the same instants the modulation index has to be updated. Due to the delay produced by the modulator and the finite computation time, the control loop represents a dead time T_d of twice the sampling interval T . The transfer

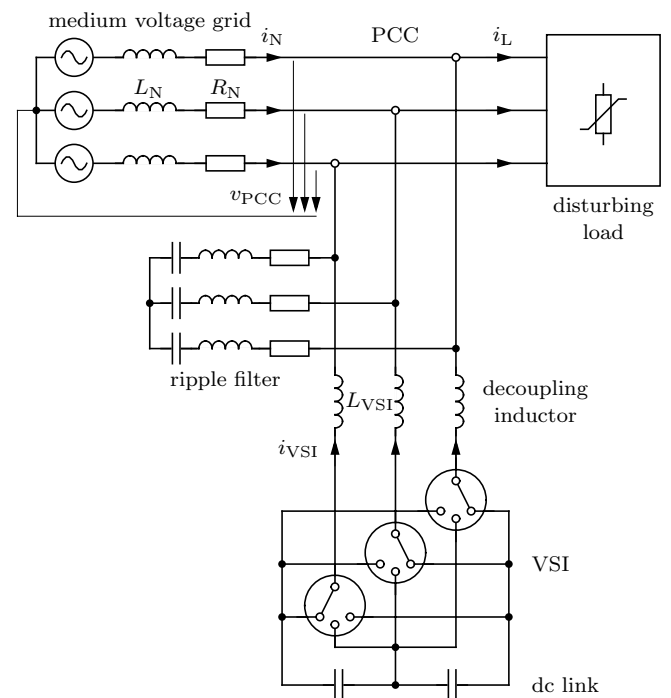


Fig. 1. Active filter configuration.

function of this closed loop is therefore:

$$G(s) = e^{-sT_d} \quad (1)$$

The VSI shall not only track stochastic transients but also compensate stationary harmonics in the load current. With the dead-beat control alone a complete compensation cannot be achieved since the inherent delay T_d causes a persistent phase error between load current i_L and VSI current i_{VSI} . At higher frequencies the VSI would even amplify certain load current harmonics. Therefore, an outer control loop is required that compensates for the the phase error. The design of this outer loop is the subject of this paper.

II. CLOSED LOOP HARMONICS COMPENSATION

In a medium voltage grid without neutral conductor all three-phase voltages and currents x_{abc} can be transformed into complex $\alpha\beta$ -phasors \vec{x} :

$$\vec{x} = x_\alpha + jx_\beta = \frac{2}{3} \left(x_a + x_b e^{j120^\circ} + x_c e^{-j120^\circ} \right) \quad (2)$$

A well-known technique to eliminate a persistent phase error in a control loop is realizing a PI controller in a rotating reference frame. This technique was first used for the control of induction machines. For active filters a controller with multiple reference frames as shown in Fig. 2 was proposed in [2], [3], and [4]. Each integrator $\frac{K_I}{s}$ ensures zero steady-state error for the respective harmonic either in positive or negative sequence. The proportional gain K_P is realized in the stationary reference frame because this signal path is not affected by the coordinate transforms.

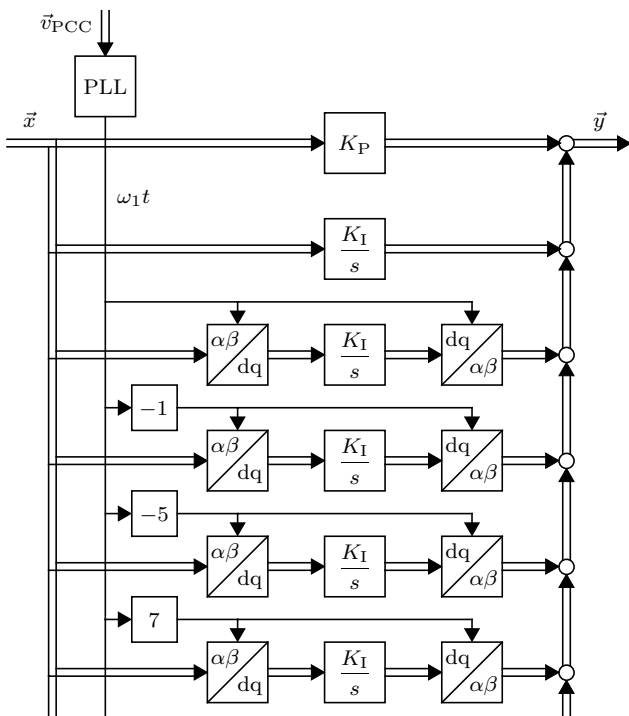


Fig. 2. Multiple reference frame controller

The drawback of this approach is the computational effort for the coordinate transforms. Two transforms are required for every harmonic component. If the active filter must also deal with unbalanced conditions the number of reference frames has to be doubled because the harmonics may appear both in positive and negative sequence.

Instead of transforming the signal continuously into various reference frames the I-controllers themselves can be transformed into the stationary reference frame as proposed in [5]. This reduces the computational effort significantly. In the stationary reference frame the former integrators $\frac{K_I}{s}$ appear as complex oscillators

$$O_\nu(s) = \frac{K_I}{s - j\omega_\nu}, \quad (3)$$

where ω_ν is the angular frequency of the ν th harmonic. The oscillators act like integrators on the magnitude of resonance frequency signals as illustrated in Fig. 3. The real component of the complex phasors is drawn in black, the imaginary component in gray.

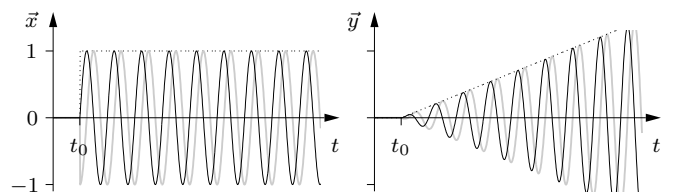


Fig. 3. Response of a complex oscillator to a resonance frequency signal.

In the stationary reference frame the control structure in Fig. 2 is characterized by the following transfer function:

$$\frac{\vec{Y}(s)}{\vec{X}(s)} = K_P + K_I \left(\frac{1}{s} + \frac{1}{s - j\omega_1} + \frac{1}{s + j\omega_1} + \dots + \frac{1}{s + j5\omega_1} + \frac{1}{s - j7\omega_1} + \dots \right) \quad (4)$$

This function can be used in a closed control loop to obtain zero steady-state error for the selected harmonics. ω_1 is the fundamental angular frequency.

III. HARMONIC ANALYSIS WITH PREFILTER

A different approach for compensating the delay of the inner dead-beat control loop is a prefilter for the reference current used in [6] and [7]. In the prefilter the harmonics are analyzed and phase shifted individually. Thus, the phase shift of the prefilter and of the dead-beat control loop cancel each other out. Fig. 4 shows the control chain.

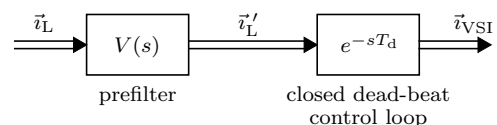


Fig. 4. Open loop control with prefilter.

A prefilter should be used where oscillators in a closed loop would interfere with grid resonances. However, the prefilter does not ensure zero steady-state error due to the open loop control. If parameter variations and disturbances change the ideal behavior of the dead-beat control loop the cancellation of harmonics remains incomplete.

A. Fourier analysis

For a harmonic analysis in the prefilter, the Fourier transform can be used. At first, the complex Fourier coefficients c_ν of all filtered harmonics must be computed from the load current phasor \vec{i}_L :

$$c_\nu = \frac{1}{T_1} \int_{t-T_1}^t \vec{i}_L(\tau) \cdot e^{-j\nu\omega_1\tau} d\tau \quad (5)$$

ν is negative for negative sequence harmonics. The window T_1 corresponds to one period of the fundamental frequency:

$$T_1 = \frac{2\pi}{\omega_1} \quad (6)$$

In order to compensate the delay T_d the phasor of each harmonic $\nu\omega_1$ must be phase shifted by $\nu\omega_1 T_d$. The Fourier coefficients c'_ν of the phase shifted harmonics are:

$$c'_\nu = e^{j\nu\omega_1 T_d} \cdot c_\nu \quad (7)$$

The harmonics not relevant for the active filter shall not appear in the reference current for the dead-beat controller. Hence, their coefficient c'_ν are set to zero. The new reference phasor \vec{i}'_L is then obtained from a reverse transform of the coefficients c'_ν :

$$\vec{i}'_L(t) = \sum_{\nu=-\infty}^{\infty} \vec{i}'_{L,\nu}(t) = \sum_{\nu=-\infty}^{\infty} c'_\nu \cdot e^{j\nu\omega_1 t} \quad (8)$$

For a single harmonic with order ν the prefilter's transfer function $F_\nu(s)$ can be calculated as

$$F_\nu(s) = \frac{\vec{i}'_{L,\nu}(s)}{\vec{i}_{L,\nu}(s)} = \frac{e^{j\nu\omega_1 T_d}}{T_1} \cdot \frac{1 - e^{-sT_1}}{s - j\nu\omega_1} \quad (9)$$

If $\nu_1, \nu_2, \dots, \nu_n$ are the orders of the filtered harmonics the complete transfer function of the prefilter has the following form:

$$F(s) = F_{\nu_1}(s) + F_{\nu_2}(s) + \dots + F_{\nu_n}(s) \quad (10)$$

In Fig. 5 the response of the transfer function $F_5(s)$ to a 5th harmonic is shown. At $t = t_0$ the magnitude of the input phasor $\vec{x}(t)$ experiences a step change from 0 to 1. The envelope of the output signal $\vec{y}(t)$ describes then a ramp-shape increase. After T_1 has passed the envelope reaches the magnitude of the input phasor and remains constant. The phase shift between input and output is too little to be seen here.

In Fig. 6 the same transfer function $F_5(s)$ is excited with a 7th harmonic. During the time T_1 after the input

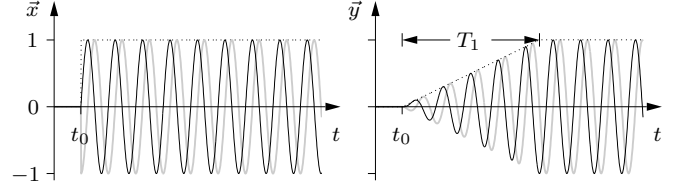


Fig. 5. Response of the Fourier transform transfer function $F_5(s)$ to a 5th harmonic.

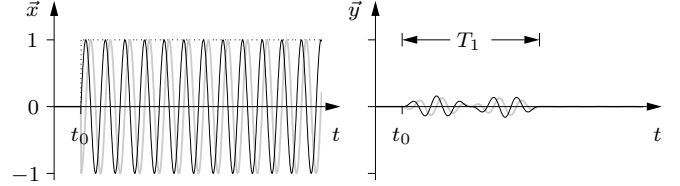


Fig. 6. Response of the Fourier transform transfer function $F_5(s)$ to a 7th harmonic.

step change the output signal describes a beat with low magnitude. Thereafter the output signal is zero.

The advantage of a Fourier analysis based prefilter is that the harmonics of the fundamental frequency can be separated independently of each other. Therefore, only those harmonics that need a phase shift have to be processed. The disadvantage of the Fourier transform is the huge computational effort, even if FFT is employed. Due to the finite impulse response a great number of multiplications and additions following every data acquisition is required. Therefore, the Fourier transform has not been applied here.

B. Bandpass filtering

As an alternative, the harmonic analysis can be performed by means of bandpasses. Compared to the Fourier transform bandpasses require only a few operations per sample. If parametrized properly they have similar performance.

As illustrated in Fig. 7 feeding back the inverted output signal of a complex oscillator $O_\nu(s)$ to its input yields a complex bandpass. At resonance frequency such a bandpass has a gain of 1 with zero phase delay. The transfer function of a bandpass tuned to the ν th harmonic is:

$$B_\nu(s) = \frac{O_\nu(s)}{1 + O_\nu(s)} = \frac{K_I}{s - j\omega_\nu + K_I} \quad (11)$$

K_I is the gain of the oscillator. It can be used to adjust the bandwidth of the bandpass. The delay T_d is compensated with a phase shifting element.

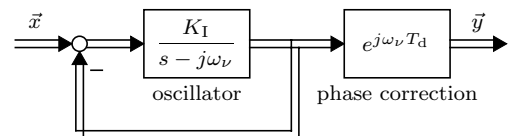


Fig. 7. Bandpass assembled from an oscillator.

Fig. 8 shows the response of a bandpass $B_5(s)$ tuned

to the 5th harmonics $5\omega_1$ and excited with resonance frequency. Here and in the following examples, the gain is set to $K_I = \frac{2}{T_1}$.

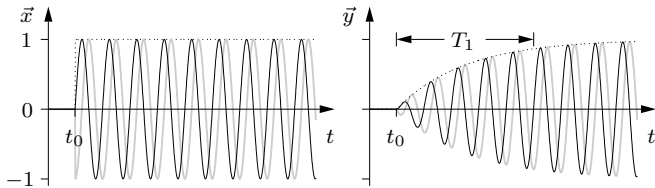


Fig. 8. Response of the bandpass $B_5(s)$ to a 5th harmonic.

Since the envelope of the output phasor $\vec{y}(t)$ describes an exponential function it matches the magnitude of the input phasor $\vec{x}(t)$ theoretically only at $t = \infty$. However, after one period T_1 of fundamental frequency the magnitudes of $\vec{x}(t)$ and $\vec{y}(t)$ are already close.

Due to the high gain K_I , single bandpasses have poor selectivity. Fig. 9 shows the response of the bandpass $B_5(s)$ excited with a 7th harmonic. Even in steady state a considerable share of the input signal remains in the output signal.

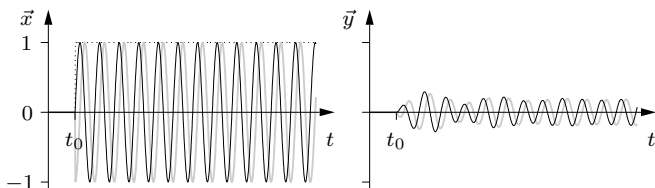


Fig. 9. Response of the isolated bandpass $B_5(s)$ to a 7th harmonic.

If a 7th harmonic oscillator $O_7(s)$ is connected in parallel to the 5th harmonic oscillator $O_5(s)$ according to Fig. 10 full selectivity for both frequencies is obtained. Due to the common feedback, a signal containing a 7th harmonic will completely disappear from the path with the 5th harmonic oscillator and vice versa. Fig. 11 shows the response $\vec{y}_5(t)$ of the 5th harmonic oscillator if the above filter structure is excited with a 7th harmonic. In steady state, the magnitude of the signal $\vec{y}_5(t)$ decreases quickly. For a 5th harmonic excitation the signal $\vec{y}_5(t)$ is similar to $\vec{y}(t)$ in Fig. 8.

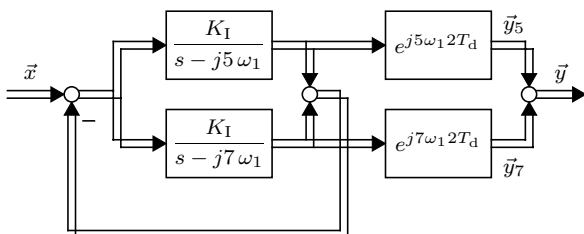


Fig. 10. Prefilter with bandpasses for the 5th and 7th harmonics.

If full selectivity is desired for all harmonics possibly present in the input signal an according number of oscillators is required. This is a disadvantage compared to the Fourier transform.

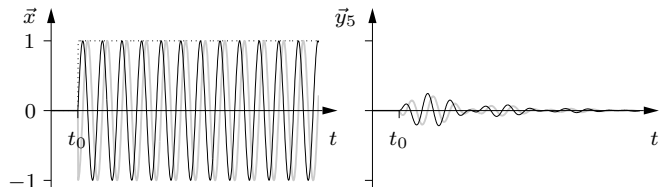


Fig. 11. Response of the 5th harmonic oscillator to a 7th harmonic.

IV. NEW CONTROL STRUCTURE

For the active filter a new control structure has been developed that combines the advantages of closed loop compensation and harmonic analysis with a prefilter. The following demands were made on the control of the active filter:

- Selected stationary harmonics are precisely compensated. After load current changes the compensation should settle within one or two periods of the fundamental frequency.
- For each harmonic the degree of compensation can be chosen. Thus, in case of impending VSI overload the compensation of individual harmonics can be reduced selectively.
- Harmonics in the PCC voltage have no repercussions on the VSI current.
- The fast tracking performance for load current transients is maintained.

The structure in Fig. 12 meets all those requirements. As a distinguishing feature from classic control loops the difference between reference and actual current is evaluated separately for every harmonic.

The load current \vec{i}_L is fed forward via the *direct path* to the inner control loop. Thus, load current transients can be tracked with the full speed of the dead-beat controller. Since the oscillators adapt relatively slowly to a new steady state they do not hinder the tracking of transients.

The oscillators in the *integral structure* are part of the closed control loop. In steady state, a harmonic matching the oscillator's resonance frequency will disappear at the oscillator input. So the harmonics in the VSI current \vec{i}_{VSI} and in the load current \vec{i}_L will be in phase. The degree of compensation is adjusted with the gain elements V_ν between 0 and 100%. To improve the loop's performance and stability an additional phase shifting element is introduced into each oscillator path. Harmonics in the PCC voltage do not appear in the VSI current if there are tuned oscillators in the integral structure.

The *bandpass structure* comprises all oscillators that would excite grid resonances in a closed loop. Here, phase shifting elements are essential due to the open loop control. The bandpasses have a common feedback that also includes the oscillator outputs of the integral structure. Hence, full selectivity for all filtered harmonics is ensured.

Active and reactive power delivered by the VSI can be adjusted with the element V_1 . V_1 is not a pure gain

but a more complex function able to separate active and reactive components. Due to the limited DC link capacitance the VSI can deliver active power only over half a period of fundamental frequency. The active component of V_1 is therefore set to zero. Furthermore, an additional PI-controller is required that minimizes the steady state DC voltage error.

V. TIME-DISCRETE IMPLEMENTATION

For the implementation of the control structure in Fig. 12 on a digital signal processor a time-discrete representation for the oscillators had to be found. Usually, Euler approximation with backward differentiation

$$\left. \frac{df}{dt} \right|_{t=kT} \approx \frac{f(kT) - f((k-1)T)}{T} \quad (12)$$

is used, where f is the time-continuous function and T the sampling interval. This would yield the following

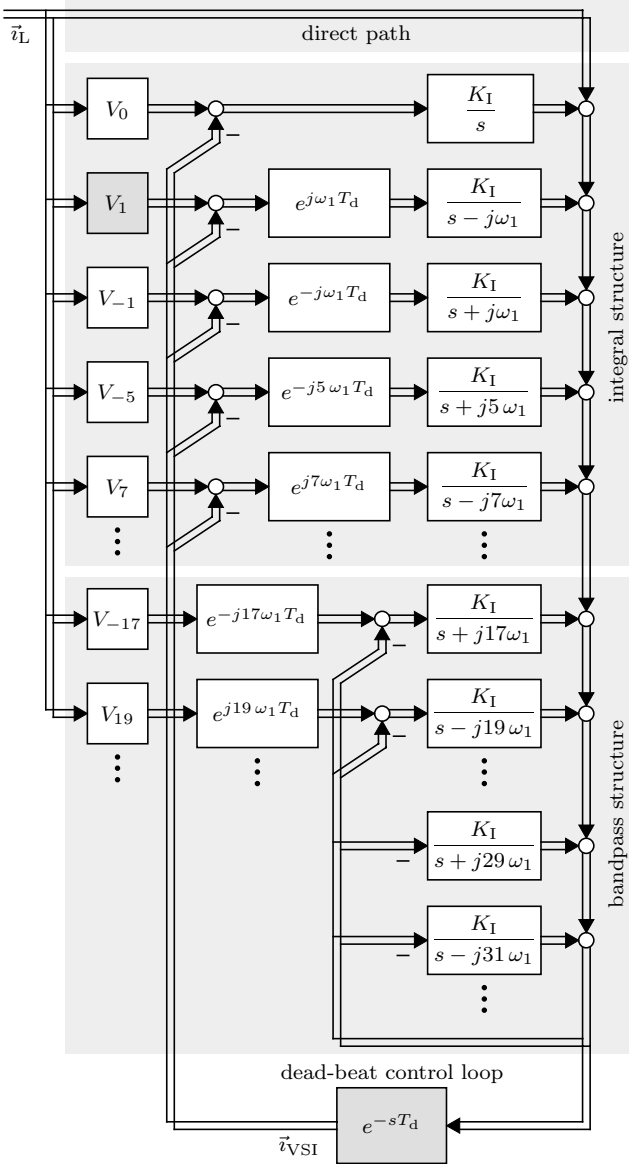


Fig. 12. Control structure for the complete compensation of stationary harmonics.

discrete oscillator function:

$$O_{\nu,z}(z) = \frac{K_I T z}{z - e^{j\omega_\nu T}} \quad (13)$$

However, in this function the output signal does not only depend on the state variable but also on the input signal. In the bandpass structure the output is fed back to the input. This would create an algebraic loop that could not be solved by the computer. Therefore, Euler approximation with forward differentiation

$$\left. \frac{df}{dt} \right|_{t=kT} \approx \frac{f((k+1)T) - f(kT)}{T} \quad (14)$$

is used here. This yields an oscillator function

$$O_{\nu,z}(z) = \frac{K_I T e^{j\omega_\nu T}}{z - e^{j\omega_\nu T}} \quad (15)$$

without direct coupling between input and output. Fig. 13 illustrates how such an oscillator is assembled from a complex storage element.

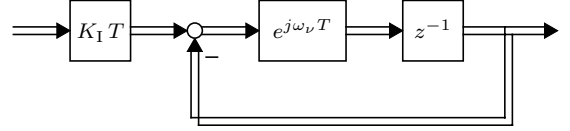


Fig. 13. Time-discrete implementation of an integrating oscillator.

VI. EXPERIMENTAL SETUP

To demonstrate the feasibility of the new control concept a 10kVA laboratory model of an active filter has been set up according to Fig. 1. The three-level VSI is build from IGBTs which operate at an average switching frequency of $F = 900$ Hz to emulate the capability of today's IGBTs. The resonant ripple filter connected in parallel to the PCC is tuned to $f_{res} = 1800$ Hz with $Q = 134$. The decoupling inductors are rated $L_{VSI} = 10\%$, the grid inductance is $L_N = 5\%$ without any additional resistance. A thyristor rectifier, switched on and off periodically, and a two-phase RL-impedance represent the fluctuating loads.

The control structure has been implemented and tested with Simulink. The laboratory model is driven by a dSPACE system which provides the means for executing the Simulink model on a TMS320C40 processor. The selection of filtered harmonics corresponds to Fig. 12. Due to the resonance frequency of the ripple filter the oscillators for the 17th harmonic and higher had to be placed in the bandpass structure.

Fig. 14 demonstrates the performance of the active filter with a six pulse rectifier load. The strong ripple of the VSI current is short-circuited by the passive filter, so it does not appear in the grid current. At $t = 20$ ms the load is switched on. The step change of the load current results in a smooth change of the grid current with little spikes caused by the initial phase error. After two periods of fundamental frequency the grid current has become virtually sinusoidal. During steady state the THD

of 22.5% in the load current is reduced to acceptable 3.9% in the grid current.

The behavior with an unsymmetrical load can be seen in Fig. 15. The load current is smoothed and symmetrized completely by the active filter. The active power pulsation is buffered by the DC link capacitors.

VII. CONCLUSIONS

A control structure for the compensation of selected stationary harmonics in active filters has been presented. The structure is based on integrating oscillators that were derived from I-controllers in rotating reference frames. Compared to FFT the oscillators show similar performance, but they are computational less intensive.

The control structure has been implemented on a real-time system and tested with a 10 kVA laboratory model. The experimental results verify the good performance of the control concept.

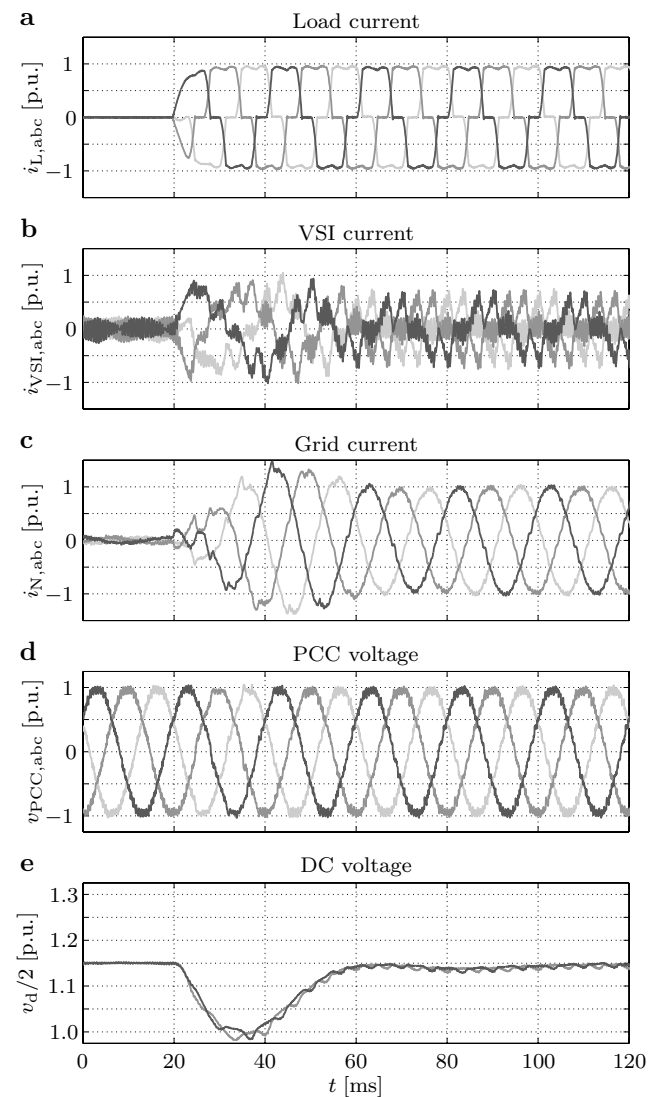


Fig. 14. Performance of the active filter with a three-phase diode rectifier as the disturbing load

REFERENCES

- [1] J. Allmeling and H. Stemmler, "A fast current control technique for active filters with low switching frequency", in *Proc. IECON 01*, Denver (USA), pp. 1125–1131, November/December 2001
- [2] C. D. Schauder and S. A. Moran, "Multiple reference frame controller for active filters and power line conditioners", *United States Patent 5,309,353*, May 1994
- [3] M. Bojrup, P. Karlsson, M. Alakula, and L. Gertmar, "A multiple rotating integrator controller for active filters", in *Proc. EPE 99*, Lausanne (Switzerland), CD-Rom, September 1999
- [4] P. Mattavelli, "A closed-loop selective harmonic compensation for active filters", in *IEEE Trans. on Industry Applications*, vol. 37, no. 1, pp. 81–89, January/February 2001
- [5] X. Yuan, J. Allmeling, W. Merk, and H. Stemmler, "Stationary frame generalized integrators for current control of active power filters with zero steady state error for current harmonics of concern under unbalanced and distorted operation conditions", in *Proc. IEEE IAS Annual Meeting*, Rome (Italy), vol. 4, pp. 2143–2150, October 2000
- [6] O. Simon, H. Spaeth, K. Juengst, and P. Komarek, "Experimental setup of a shunt active filter using a superconducting magnetic energy storage", in *Proc. EPE 97*, Trondheim (Norway), vol. 1, pp. 447–452, September 1997
- [7] S. Mariethoz and A. Rufer, "Vers le traitement numérique de l'énergie – le filtrage actif d'harmoniques par DSP", in *Bulletin ASE/AES*, vol. 90, no. 25, pp. 28–32, December 1999

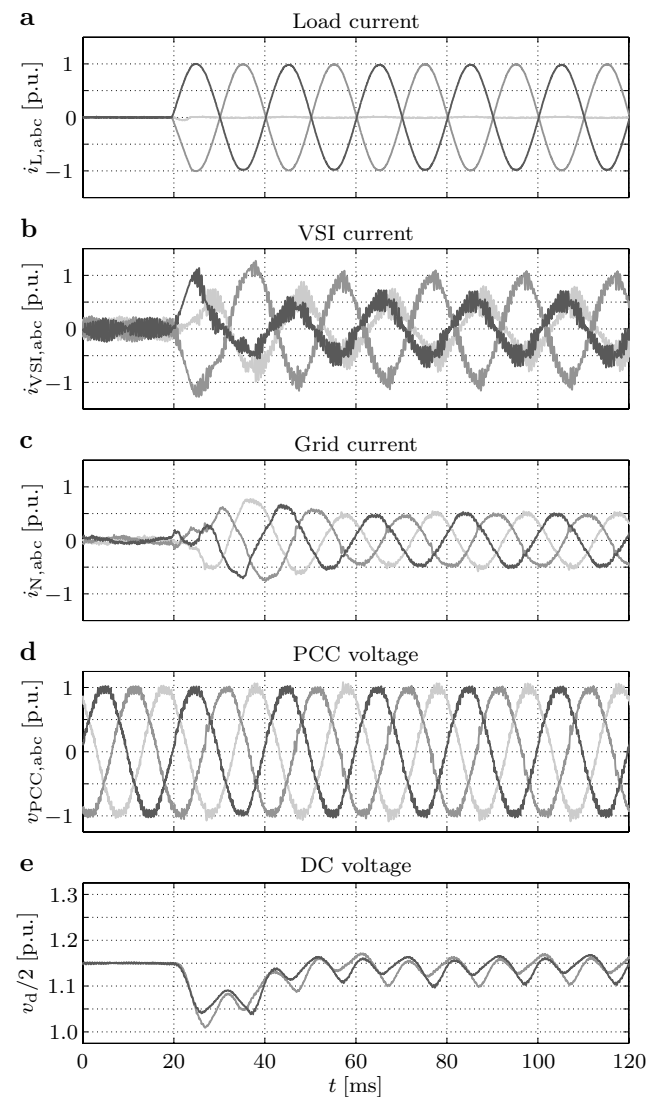


Fig. 15. Performance of the active filter with an unsymmetrical disturbing load